Available online at www.sciencedirect.com
SCIENCE DIRECT®
Journal of Solid State Chemistry 177 (2004) 4282–4285
JOURNAL OF SOLID STATE CHEMISTRY
www.elsevier.com/locate/jssc

Proton dynamics in superionic phase of $Tl_3H(SO_4)_2$

Yasumitsu Matsuo*, Keisuke Takahashi, Junko Hatori, Seiichiro Ikehata

Faculty of Science, Department of Applied Physics, Tokyo University of Science, 1-3 Kagurazaka, Shinjyuku-ku, Tokyo 162-8601, Japan

Received 4 February 2004; received in revised form 26 July 2004; accepted 10 August 2004

Abstract

Electrical properties and ^{1}H-NMR absorption line have been measured, in order to investigate proton dynamics in a superionic phase in $Tl_3H(SO_4)_2$. From the measurement of the thermoelectric power, it is found that a majority carrier in electrical conductivity is a proton. Moreover, from ^{1}H-NMR measurement it is also found that the activation energy 0.33 eV of the hopping motion of protons is close to 0.38 eV as observed in the electrical conductivity measurement. These results indicate that the electrical conductivity in the superionic phase is caused by the hopping motion of protons accompanied by the breaking of the hydrogen bonds.

PACS: 66.30.Hs; 77.80.Dj; 77.90.+k

Keywords: $Tl_3H(SO_4)_2$; Superionic conductor; NMR; Electrical conductivity; Proton dynamics

1. Introduction

Recently, many efforts in the studies on zero-dimensional hydrogen-bonded $M_3H(XO_4)_2$ (M: K, Rb, Cs, NH_4; X: S, Se)-type compounds have been devoted in conjunction with the development of fuel cell [1-12]. The $M_3H(XO_4)_2$-type compounds undergo a superionic phase transition from a low-temperature ferroelastic phase to a high-temperature paraelastic phase. The thermal rotational displacement of XO_4 tetrahedrons observed at the superionic phase transition is closely related to the appearance of the superionic phase. Therefore, it was expected for $M_3H(XO_4)_2$-type compounds that the superionic phase transition is observed at higher temperature such as 400 K.

However, recently, it was found from dielectric and thermal studies that the $Tl_3H(SO_4)_2$ crystal, which is one of $M_3H(XO_4)_2$-type compounds, undergoes the superionic phase transition at 239 K[13]. That is, this crystal becomes a superionic conductor at room temperature. This crystal belongs to the trigonal system with a space group of $R\bar{3}m$ at room temperature [14]. The most interesting feature of this structure is that the disordered states of oxygen, which rotates between three equivalent sites accompanied by the breaking of the hydrogen bond, exist in the superionic phase. Therefore, in $Tl_3H(SO_4)_2$, it is deduced that even at room temperature the breaking and rearrangement of the hydrogen bond are iterated accompanied by the rotational displacement of SO_4 tetrahedrons. The investigation on the superionic conduction in $Tl_3H(SO_4)_2$ will lead to the further understanding of the role of a proton in electrical conductivity in the superionic phase of $M_3H(XO_4)_2$-type compounds. In the present paper, we report the experimental results of the thermal, electrical and ^{1}H-NMR measurements and discuss the role of a proton in the superionic phase transition.

2. Experimental procedure

The $Tl_3H(SO_4)_2$ crystals were grown by the slow evaporation method from an aqueous solution of

*Corresponding author. Fax: +81-3-3260-4772.
E-mail address: ymatsuo@rs.kagu.tus.ac.jp (Y. Matsuo).

0022-4596/$ - see front matter © 2004 Elsevier Inc. All rights reserved.
doi:10.1016/j.jssc.2004.08.028

Tl_2SO_4 and H_2SO_4 with a molar ratio of Tl_2SO_4: $H_2SO_4 = 3{:}2$ at 313 K. The single crystals form a hexagonal thin plate with the predominant (001) faces and are transparent. Measurements of the electrical conductivity were carried out by using a polycrystalline pressed pellet sample below room temperature in the frequency range from 100 to 10 kHz using an LCR meter (4284A: Hewlett Packard Co. Ltd.). Measurements of thermoelectric power were carried out with the experimental arrangement as shown in the previous paper [15]. The NMR absorption lines were observed by the Q-meter detective method at the resonance frequency of 10.6 MHz with powder specimens.

3. Results and discussion

Fig. 1 shows the frequency f dependence of the imaginary part of dielectric constant ε'' at various temperatures. We can see clearly that, in the frequency range from 100 Hz to 10 kHz, $\log \varepsilon''$ is proportional to $\log f$ with the following equation:

$$\varepsilon'' = \frac{\sigma}{2\pi\varepsilon_0 f}. \tag{3.1}$$

Here, σ is the static electrical conductivity and ε_0 the permittivity of vacuum. Therefore, we can estimate the temperature dependence of the static electrical conductivity σ by analyzing the frequency dependence of ε'' at various temperatures.

Fig. 2 shows the temperature dependence of σ as a plot of $\log \sigma T$ against inverse temperature. As shown in Fig. 2, σ shows anomalous behaviors at $T_{\mathrm{I-II}} = 267$ K, $T_{\mathrm{II-III}} = 239$ K and $T_{\mathrm{III-IV}} = 196$ K. At the superionic phase transition temperature of $T_{\mathrm{II-III}}$ σ steeply increases and becomes about 10^{-4} S/cm at room temperature. Moreover, it is also noted that $\log \sigma T$ is proportional to $1/T$ with increasing temperature in the superionic phases. From this result, we calculate the activation energies for the superionic phases I and II using the Arrhenius' equation

$$\sigma = A'/T \exp(-E_a/k_B T), \tag{3.2}$$

where A' is the pre-exponential factor and k_B is Bolzmann's constant. The activation energies in the phases I and II are calculated to be 0.34 and 0.38 eV, respectively.

In Fig. 3, the thermoelectromotive force ΔV is shown as a function of temperature difference ΔT in the

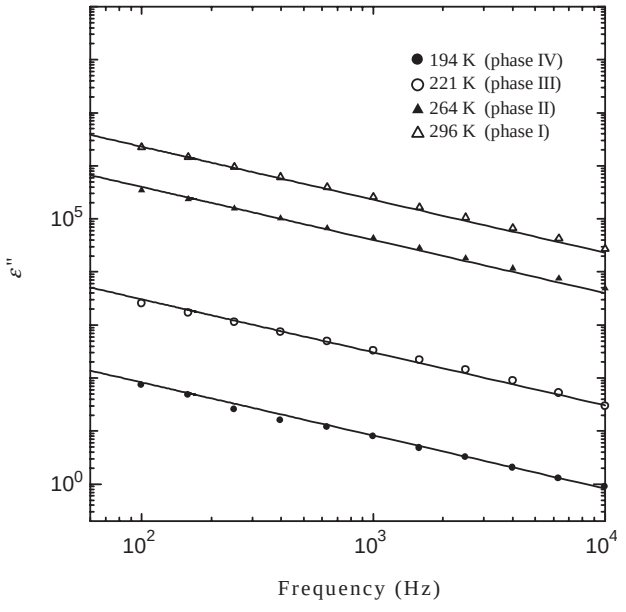

Fig. 1. Frequency dependence of ε''. Solid lines show the fitted ones using Eq. (3.1).

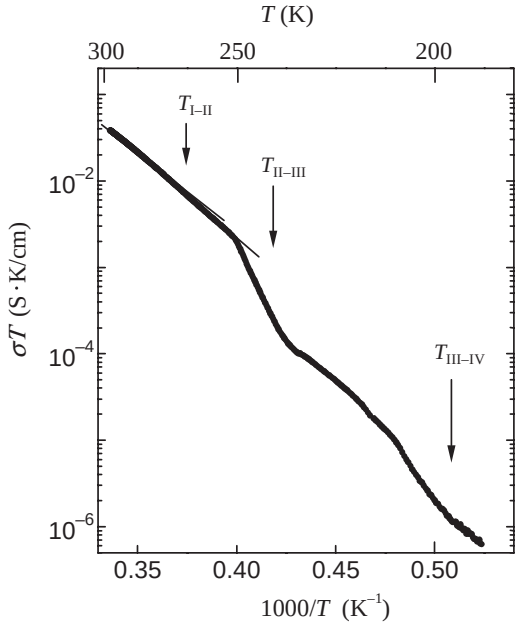

Fig. 2. $\sigma T - 1/T$ characteristic.

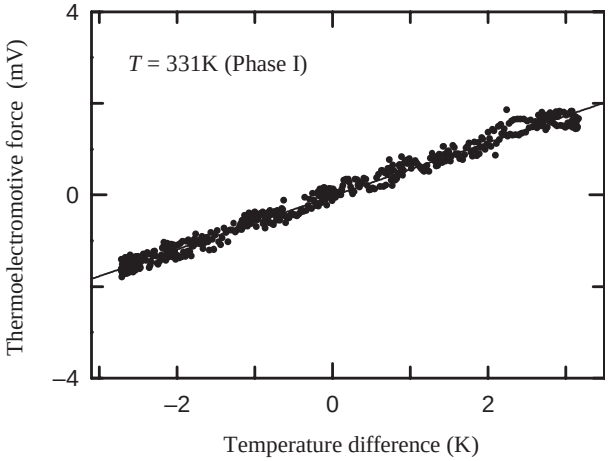

Fig. 3. $\Delta V - \Delta T$ characteristic.

superionic phase of 331 K. It is evident that the absolute value of the thermoelectromotive force $|\Delta V|$ increases linearly with the increase of $|\Delta T|$.

Moreover, it is also noted that the sign of the thermoelectric power $S=(\Delta V/\Delta T)$ is a positive. This result indicates that the majority carrier in electrical conductivity in the superionic phase is a proton.

Fig. 4 shows the ^{1}H-NMR absorption lines at various temperatures. As shown in Fig. 4, the ^{1}H-NMR absorption lines show the broad ones in the phases III, IV and V compared with those in the phases I and II. Thus, the ^{1}H-NMR absorption line becomes sharp above $T_{\mathrm{II–III}}$. Moreover, the shape of the NMR absorption lines in the phases III, IV and V are described well with the Gaussian curve that corresponds to the NMR line for rigid lattice. On the other hand, the NMR absorption lines observed above $T_{\mathrm{II–III}}$ are described with the functional form mixed with the Gaussian curve and the Lorenzian curve. It is well known that the NMR absorption line with the Lorenzian curve is caused by the existence of mobile protons. Therefore, this result indicates that mobile protons exist above $T_{\mathrm{II–III}}$.

It is also noted that the ^{1}H-NMR linewidth becomes narrow above $T_{\mathrm{II–III}}$ drastically. In order to examine the narrowing of ^{1}H-NMR absorption line more in detail, we show the temperature dependence of the second moment M_2 in Fig. 5. The second moment is closely related with the linewidth of the ^{1}H-NMR absorption line. The second moment M_2 is directly calculated from the measured NMR absorption lines at various temperatures using the following equation:

$$M_2 = \frac{\int_{-\infty}^{\infty}(H-H_0)^2 f(H-H_0)\,\mathrm{d}H}{\int_{-\infty}^{\infty} f(H-H_0)\,\mathrm{d}H},$$

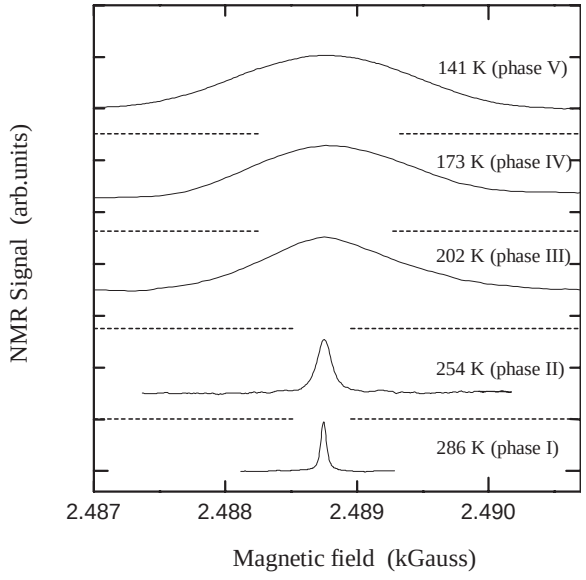

Fig. 4. ^{1}H-NMR absorption lines at various temperatures.

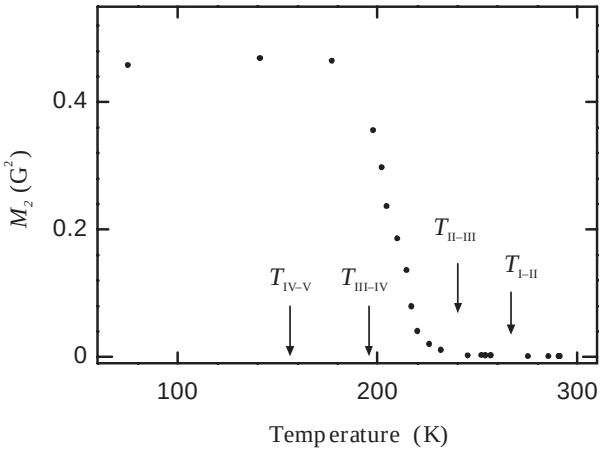

Fig. 5. Temperature dependence of second moment M_2.

where H_0 and H are the resonance magnetic field and the external magnetic field, respectively. The function $f(H)$ means the measured NMR absorption line.

The second moment M_2 is approximately 0.47 G^2 below 190 K, which begins to decrease above approximately 190 K with increasing temperature and becomes below 0.01 G^2 in the superionic phases I and II. The decrease in M_2 results from the motional narrowing of the ^{1}H-NMR absorption line, because the mobile proton leads to an averaging of the local field produced by the magnetic dipole–dipole interaction of protons. This result indicates that the hopping motion of protons begins above 190 K and that in the superionic phases protons move with the hopping rate that is fast enough to narrow the ^{1}H-NMR absorption line. As described in the introduction, the oxygen closely related with the hydrogen bond in the SO_4 tetrahedrons moves between three equivalent sites. Considering this result, the hopping motion of protons is caused by the breaking and rearrangement of the hydrogen bonds accompanied by the hopping motion of the oxygen between three equivalent sites. It is also noted that the onset of the decrease in M_2 appears below the superionic phase transition. It is known that the hopping motion of protons is observed even below the superionic phase in the isomorphic $Rb_3H(SeO_4)_2$ crystal, accompanied by the growth of the micro-domain structure [3,9]. Therefore, this decrease in M_2 observed below $T_{\mathrm{II–III}}$ is caused by the precursor effect of the hopping motion of protons in the superionic phase of phase II (that is, we can obtain proton motion in the phase II by analyzing the decrease in M_2 observed below $T_{\mathrm{II–III}}$). Moreover we note that at $T_{\mathrm{I–II}}$ M_2 decreases from 2.06×10^{-3} G^2 at 257 K to 4.47×10^{-4} G^2 at 276 K with increasing temperature. It seems that the decrease of M_2 at $T_{\mathrm{I–II}}$ is caused by the increase in mobility of proton accompanied by the phase transition or the increase in the conducting path of proton such as the change from

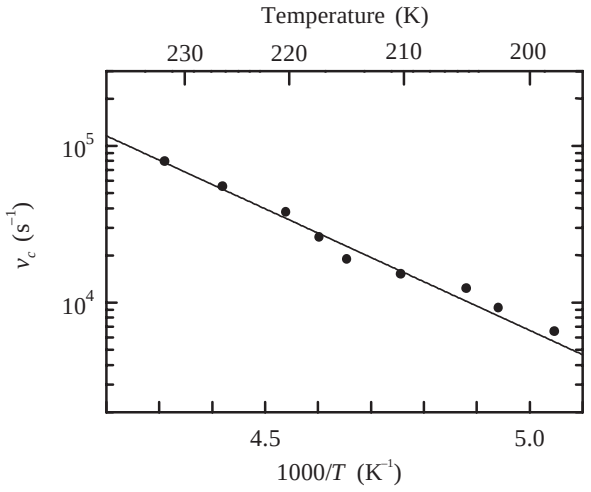

Fig. 6. Temperature dependence of the correlation frequency v_c.

the two-dimensional conduction of proton to the three-dimensional conduction.

Furthermore, an analysis of the second moment makes it possible to determine the correlation frequency v_c for the hopping motion of protons, which leads to the narrowing of the NMR absorption line. The analysis was carried out using equation [16]:

$$v_c = \frac{\gamma}{2\pi} \frac{\alpha\sqrt{M_2}}{\tan\left(\frac{\pi}{2}\frac{M_2 - M_2^H}{M_2^L - M_2^H}\right)}, \tag{3.4}$$

which describes the temperature dependence of v_c obtained from various values of M_2. Here, M_2^L and M_2^H are the second moments before and after narrowing, respectively. The constant α is $(8\ln 2)^{-1}$. The correlation time is assumed to obey the Arrhenius' relation

$$v_c = v_0 \exp(-E_a/k_B T) \tag{3.5}$$

so that we can obtain the correlation frequency for high-temperature limit frequency v_0 and the activation energy E_a of the hopping motion of protons. Fig. 6 shows the temperature dependence of the correlation frequency v_c obtained for the hopping motion of protons. It is evident that log v_c is proportional to $1/T$. From this result, we find $v_0 = 7.7 \times 10^{10}\,s^{-1}$ and $E_a = 0.33$ eV.

It is known that the activation energies of the $M_3H(XO_4)_2$-type compounds in the superionic phase become 0.26–0.39 eV in the a–b plane of the hexagonal system in the super-ionic phase and become 0.40–0.61 eV along the c-axis [2]. The activation energy obtained from the measurement of electrical conductivity in the polycrystalline pressed pellet sample of $Tl_3H(SO_4)_2$ is 0.38 eV in the phase II. In NMR measurement, we also used the powder sample and therefore obtain the activation energy of 0.33 eV averaged on all directions. This value is close to that obtained from the electrical conductivity measurement. From these results it is deduced that the hopping motion of protons, which is caused by the breaking and rearrangement of the hydrogen bonds, leads to the electrical conductivity in the superionic phase.

4. Summary

We have measured the thermoelectric power, electrical conductivity and ^{1}H-NMR absorption line and have investigated the role in a proton in electrical conductivity on $Tl_3H(SO_4)_2$. We have obtained from the thermoelectric power $S = (\Delta V/\Delta T)$ that the majority carrier in electrical conductivity in the superionic phase is a proton. Moreover it is also found from the analyses of the second moment of ^{1}H-NMR absorption line that the activation energy of 0.33 eV for the hopping motion of protons in the superionic phase (phase II) is close to that of 0.38 eV observed in the electrical conductivity measurement using the polycrystalline pressed pellet sample. These results indicate that the electrical conductivity of the $Tl_3H(SO_4)_2$ crystal observed in the superionic phase results from the hopping motion of protons accompanied by the breaking and rearrangement of the hydrogen bonds.

References

[1] Y. Matsuo, K. Takahashi, K. Hisada, S. Ikehata, J. Phys. Soc. Japan 68 (1999) 2965.
[2] A. Pawlowski, Cz. Pawlaczyk, B. Hilczer, Solid State Ionics 81 (1990) 17.
[3] Y. Matsuo, K. Takahashi, S. Ikehata, J. Phys. Soc. Japan 70 (2001) 2934.
[4] C. Abramic, J. Dolinsek, R. Blinc, Phys. Rev. B 42 (1990) 442.
[5] A. Bohn, R. Melzer, T. Sonntag, R.E. Lechner, G. Schuck, K. Langer, Solid State Ionics 77 (1995) 111.
[6] B.V. Merinov, Solid State Ionics 84 (1996) 89.
[7] M. Komukae, K. Sakata, T. Osaka, Y. Makita, J. Phys. Soc. Japan 63 (1994) 1009.
[8] T. Ito, H. Kamimura, J. Phys. Soc. Japan 67 (1998) 1999.
[9] H. Kamimura, S. Watanabe, Philos. Mag. B 81 (2001) 1011.
[10] Y. Matsuo, J. Hatori, Y. Nakashima, S. Ikehata, Solid State Commun. 130 (2004) 269.
[11] S.M. Haile, D.A. Boysen, C.R.I. Chisholm, R.B. Merle, Nature 410 (2001) 910.
[12] T. Norby, Nature 410 (2001) 877.
[13] Y. Matsuo, K. Takahashi, S. Ikehata, Solid State Commun. 120 (2001) 85.
[14] Y. Matsuo, S. Kawachi, Y. Shimizu, S. Ikehata, Acta Cryst. C 58 (2002) i92.
[15] Y. Matsuo, K. Takahashi, S. Ikehata, Solid State Commun. 119 (2001) 79.
[16] A. Abragam, The Principles of Nuclear Magnetism, The Clarendon Press, 1961 (Chapter 10).